

**The Optical Gravitational Lensing Experiment.  
Cepheids in the Magellanic Clouds.  
I. Double-Mode Cepheids  
in the Small Magellanic Cloud\***

**A. Udalski<sup>1</sup>, I. Soszyński<sup>1</sup>,  
M. Szymański<sup>1</sup>, M. Kubiak<sup>1</sup>, G. Pietrzyński<sup>1</sup>,  
P. Woźniak<sup>2</sup>, and K. Żebruń<sup>1</sup>**

<sup>1</sup>Warsaw University Observatory, Al. Ujazdowskie 4, 00-478 Warszawa,  
Poland

e-mail: (udalski,soszynsk,msz,mk,pietrzyn,zebrun)@sirius.astro.uw.edu.pl

<sup>2</sup> Princeton University Observatory, Princeton, NJ 08544-1001, USA  
e-mail: wozniak@astro.princeton.edu

ABSTRACT

We present a sample of 93 double-mode Cepheids detected in the 2.4 square degree area in the central part of the SMC. 23 stars from the sample pulsate in the fundamental mode and the first overtone while 70 objects are the first and second overtone pulsators. This is the largest sample of such type Cepheids detected in one environment so far.

We analyze period ratio of double-mode Cepheids, Fourier parameters of decomposition of the light curves of these objects and also  $V - I$  color distribution of Cepheids in the observed fields. We also find one object which is probably a blend, either physical or optical, of two Cepheids pulsating in the fundamental mode.

## 1 Introduction

Microensing searches for dark matter in the Galaxy provide an unique by-product – huge databases of precise photometric measurements of tens million stars in the Magellanic Clouds and dense Galactic fields. The measurements span a few years and are ideally suited for variable star study. One of the group of variable stars profiting a lot from microensing surveys data are pulsating variable stars. The Magellanic Clouds offer an ideal sample

---

\*Based on observations obtained with the 1.3 m Warsaw telescope at the Las Campanas Observatory of the Carnegie Institution of Washington.

of those stars due to their large population there and approximately the same distance. Unfortunately, they have been neglected photometrically for years.

About 1400 Cepheids were identified in the Large Magellanic Cloud by the MACHO microlensing team (Alcock *et al.* 1995). The majority of objects are regular single-mode pulsators. Alcock *et al.* (1995) also presented a sample of 45 double-mode Cepheids identified among detected objects. The double-mode Cepheids (called sometimes beat Cepheids) pulsate simultaneously in two radial modes: either fundamental and first overtone (FU/FO) or first and second overtones (FO/SO). The double-mode Cepheids are relatively rare, only fourteen were identified in the Galaxy so far (Pardo and Poretti 1997). Large sample of double-mode Cepheids from the LMC, increased later to 75 objects, allowed for more detailed study of properties of these objects (Alcock *et al.* 1999).

The double-mode Cepheids were also identified in the Small Magellanic Cloud. 27 object sample was reported by the MACHO team (Alcock *et al.* 1997) and 11 object sample by the EROS team (Beaulieu *et al.* 1997). The sample of the SMC Cepheids is very important because smaller metallicity of the SMC allows to study dependence of pulsation properties of double-mode Cepheids on their metallicity.

The Magellanic Clouds were included to the observing targets of the Optical Gravitational Lensing Experiment (OGLE) microlensing search at the beginning of the second phase of the project, OGLE-II, in January 1997 (Udalski, Kubiak and Szymański 1997). After two years of constant monitoring of the Magellanic Clouds, the photometric databases of the OGLE project are complete enough to allow for search for Cepheids in the Magellanic Clouds. In this paper, first of the series on Cepheid variable stars in the Magellanic Clouds, we present results of the search for double-mode Cepheids in the central regions of the SMC leading to discovery of 93 such objects – the largest sample of double-mode Cepheids detected so far.

## 2 Observations

All observations presented in this paper were carried out with the 1.3-m Warsaw telescope at the Las Campanas Observatory, Chile, which is operated by the Carnegie Institution of Washington, during the second phase of the OGLE experiment. The telescope was equipped with the "first generation" camera with a SITE  $2048 \times 2048$  CCD detector working in the drift-scan

mode. The pixel size was  $24 \mu\text{m}$  giving the  $0.417 \text{ arcsec/pixel}$  scale. Observations of the SMC were performed in the "slow" reading mode of the CCD detector with the gain  $3.8 \text{ e}^-/\text{ADU}$  and readout noise about  $5.4 \text{ e}^-$ . Details of the instrumentation setup can be found in Udalski, Kubiak and Szymański (1997).

Observations of the SMC started on June 26, 1997. As the microlensing search is planned to last for a few years, observations of selected fields will be continued during the following seasons. In this paper we present data collected up to March 4, 1998. Observations are obtained in the standard *BVI*-bands with majority of measurements made in the *I*-band.

Photometric data collected in the course of the first observing season of the SMC for 11 fields (SMC\_SC1–SMC\_SC11) covered about 2.4 square degree of the central parts of the SMC and were used to construct the *BVI* photometric maps of the SMC (Udalski *et al.* 1998a). The reader is referred to that paper for more details about methods of data reduction, tests on quality of photometric data, astrometry, location of observed fields etc.

### 3 Selection of Double-Mode Cepheids

The search for variable objects in 11 SMC fields was performed using observations in the *I*-band in which majority of observations was obtained. Typically about 160–200 epochs were available for each analyzed object with the lower limit set to 50. The mean *I*-band magnitude of objects was limited to  $I < 20 \text{ mag}$ . Candidates for variable stars were selected based on comparison of the standard deviation of all individual measurements of a star with typical standard deviation for stars of similar brightness. Light curves of selected candidates were then searched for periodicity using the AoV algorithm (Schwarzenberg-Czerny 1989).

Candidates for Cepheids were selected from the entire sample of variable stars based on visual inspection of the light curves and location in the color-magnitude diagram (CMD) within the area limited by  $I < 18.5 \text{ mag}$  and  $0.25 < (V - I) < 1.3 \text{ mag}$ . Several objects located outside this region but with evident Cepheid light curves were also included to this sample (*e.g.*, highly reddened Cepheids). In total more than 2300 Cepheid candidates were found in the 2.4 square degree area of the SMC bar. The catalog of all objects will be presented in the following papers of this series.

Selection of double-mode Cepheids was performed in two stages. First, in the preliminary search, we used results of the general variable star search

described above. The mean light curve folded with the AoV period of each Cepheid candidate was fitted by high order polynomial and subtracted from the light curve. Double-mode Cepheids fold usually with the higher amplitude periodicity displaying abnormally large scatter in the light curve. The residuals were then searched for periodic signal and, if detected, such a candidate was marked for further analysis. Then a histogram of the ratio of the shorter to the longer period of selected double-mode Cepheid candidates was constructed. It exhibited two clear sharp peaks corresponding to the ratio of the first overtone to the fundamental period,  $\approx 0.735$ , and the second to the first overtone period,  $\approx 0.805$ , in good agreement with Alcock *et al.* (1997). The list of the double-mode Cepheid candidates from this search included stars having the period ratio within  $\pm 0.02$  from these values – the range wide enough to avoid missing potential outliers.

The second, final search for double-mode Cepheids was performed using the CLEAN algorithm of period determination (Roberts, Lehár and Dreher 1987). All 2300 objects from the Cepheid candidate list were subjected to the CLEAN period analysis. Having well established limits for the period ratio of double-mode Cepheids from the preliminary analysis, only those objects which exhibited suitable period ratio ( $\pm 0.015$ ) between the highest peak in the power spectrum and one of the next four strongest peaks were further analyzed. The final list of the double-mode Cepheid candidates presented in this paper was obtained after careful visual inspection of the CLEAN power spectra of each object.

## 4 Double-Mode Cepheids in the SMC

Double-mode Cepheids detected in the central area of the SMC are listed in Tables 1 and 2. 95 objects were detected but 93 of them are unique. Two stars are located in the overlapping regions between fields and they were discovered independently in each field. Table 1 contains systems which pulsate in the fundamental and first overtone modes while Table 2 – objects pulsating in the first and second overtones. Basic parameters of each star: right ascension and declination (J2000), the mean intensity weighted *I*-band magnitude,  $(B - V)$  and  $(V - I)$  colors, both periods and their ratio are provided. Accuracy of periods is about  $7 \cdot 10^{-5}P$ . Finding charts for all objects are presented in Appendix A. The size of the *I*-band subframes is  $60 \times 60$  arcsec; North is up and East to the left.

Appendices B and C show the light curves of FU/FO and FO/SO pul-

Table 1  
FU/FO Double-Mode Cepheids in the SMC

Field	Star No.	RA(J2000)	DEC(J2000)	$P_{FO}$ [days]	$R_{21}^{FO}$	$\phi_{21}^{FO}$	$\phi_{31}^{FO}$	$P_{FU}$ [days]	$R_{21}^{FU}$	$\phi_{21}^{FU}$	$\phi_{31}^{FU}$	$P_{FO}/P_{FU}$	$I$ [mag]	$B - V$ [mag]	$V - I$ [mag]	Remarks
SMC_SC1	35550	0 <sup>h</sup> 37 <sup>m</sup> 20 <sup>s</sup> .12	-73°39'33".1	1.05420	0.206	4.356	2.546	1.43146	0.000	-	-	0.73645	17.095	0.404	0.589	
SMC_SC1	60587	0 <sup>h</sup> 38 <sup>m</sup> 31 <sup>s</sup> .23	-73°49'20".4	0.81481	0.255	3.915	1.504	1.10441	0.091	3.274	-	0.73778	17.246	0.458	0.582	
SMC_SC2	61720	0 <sup>h</sup> 41 <sup>m</sup> 28 <sup>s</sup> .84	-73°23'00".5	1.31403	0.231	4.866	2.575	1.79017	0.196	4.429	-	0.73403	16.638	0.413	0.660	M
SMC_SC4	56827	0 <sup>h</sup> 46 <sup>m</sup> 48 <sup>s</sup> .49	-73°24'39".2	1.29792	0.165	4.646	-	1.77773	0.140	4.051	-	0.73010	16.927	0.511	0.703	
SMC_SC4	75443	0 <sup>h</sup> 46 <sup>m</sup> 12 <sup>s</sup> .62	-73°06'14".0	1.03846	0.193	4.335	-	1.41624	0.000	-	-	0.73325	17.453	0.708	0.917	
SMC_SC4	91592	0 <sup>h</sup> 46 <sup>m</sup> 12 <sup>s</sup> .86	-72°46'56".4	1.58163	0.178	5.078	-	2.16767	0.109	4.334	-	0.72965	16.207	0.520	0.621	
SMC_SC4	145181	0 <sup>h</sup> 47 <sup>m</sup> 38 <sup>s</sup> .51	-72°42'45".3	1.26823	0.208	4.204	0.748	1.71360	0.187	4.741	-	0.74010	15.379	0.411	0.504	
SMC_SC4	175210	0 <sup>h</sup> 48 <sup>m</sup> 21 <sup>s</sup> .56	-73°07'17".3	1.34951	0.246	4.725	3.306	1.84077	0.227	4.442	-	0.73312	16.080	0.387	0.649	
SMC_SC5	38289	0 <sup>h</sup> 48 <sup>m</sup> 47 <sup>s</sup> .13	-73°05'35".7	1.54316	0.179	4.873	3.724	2.09712	0.139	4.410	-	0.73585	17.180	0.608	0.975	
SMC_SC5	117506	0 <sup>h</sup> 49 <sup>m</sup> 33 <sup>s</sup> .33	-73°06'32".9	1.66881	0.147	4.885	3.841	2.28834	0.128	4.601	-	0.72927	16.439	0.507	0.698	
SMC_SC5	155033	0 <sup>h</sup> 49 <sup>m</sup> 54 <sup>s</sup> .21	-72°40'54".0	1.63619	0.118	5.237	4.697	2.24323	0.172	4.855	-	0.72939	16.187	0.464	0.685	
SMC_SC5	219993	0 <sup>h</sup> 50 <sup>m</sup> 44 <sup>s</sup> .08	-72°53'06".7	1.63153	0.161	5.168	3.826	2.23121	0.213	4.505	2.506	0.73123	16.501	0.513	0.750	
SMC_SC6	49262	0 <sup>h</sup> 52 <sup>m</sup> 10 <sup>s</sup> .75	-72°55'28".5	1.47521	0.220	4.906	3.111	2.02103	0.168	4.380	-	0.72993	16.514	0.357	0.702	M
SMC_SC6	77317	0 <sup>h</sup> 51 <sup>m</sup> 57 <sup>s</sup> .98	-72°40'39".0	1.22115	0.179	4.828	3.024	1.66233	0.140	3.766	-	0.73460	16.749	0.608	0.671	M
SMC_SC6	221538	0 <sup>h</sup> 53 <sup>m</sup> 13 <sup>s</sup> .90	-72°52'42".6	1.58721	0.174	5.083	3.197	2.18075	0.158	4.548	-	0.72783	16.358	0.498	0.663	M
SMC_SC7	57228	0 <sup>h</sup> 55 <sup>m</sup> 11 <sup>s</sup> .37	-72°38'19".0	1.40258	0.253	4.794	3.466	1.91162	0.184	4.464	2.944	0.73371	16.589	0.488	0.670	
SMC_SC7	70881	0 <sup>h</sup> 54 <sup>m</sup> 57 <sup>s</sup> .86	-72°27'08".8	1.34302	0.191	4.630	3.362	1.83351	0.153	4.591	-	0.73249	16.149	0.427	0.576	
SMC_SC7	164739	0 <sup>h</sup> 56 <sup>m</sup> 18 <sup>s</sup> .44	-73°03'46".7	1.28429	0.190	4.448	2.970	1.75401	0.000	-	-	0.73220	16.619	0.424	0.597	U
SMC_SC7	197655	0 <sup>h</sup> 56 <sup>m</sup> 11 <sup>s</sup> .62	-72°34'52".5	1.50270	0.189	4.824	-	2.05474	0.153	4.476	-	0.73133	16.525	0.482	0.645	
SMC_SC7	259596	0 <sup>h</sup> 57 <sup>m</sup> 19 <sup>s</sup> .80	-72°35'11".9	0.64372	0.149	3.676	-	0.86343	0.000	-	-	0.74554	17.753	0.526	0.706	
SMC_SC8	30629	0 <sup>h</sup> 58 <sup>m</sup> 06 <sup>s</sup> .52	-72°37'11".1	1.37282	0.253	4.593	3.302	1.87704	0.149	3.537	-	0.73137	16.471	0.556	0.618	
SMC_SC8	195810	1 <sup>h</sup> 00 <sup>m</sup> 06 <sup>s</sup> .37	-72°30'04".8	1.61709	0.171	5.039	-	2.22111	0.093	3.888	-	0.72805	16.190	0.478	0.661	
SMC_SC10	128768	1 <sup>h</sup> 06 <sup>m</sup> 17 <sup>s</sup> .71	-72°24'42".7	1.67025	0.223	4.965	2.925	2.28535	0.204	4.531	-	0.73085	16.198	0.505	0.698	M
SMC_SC11	24037	1 <sup>h</sup> 06 <sup>m</sup> 17 <sup>s</sup> .71	-72°24'42".9	1.67035	0.214	4.990	3.502	2.28610	0.191	4.620	-	0.73065	16.210	0.494	0.695	S

Remarks: M: Double-mode Cepheid reported by MACHO (Alcock *et al.* 1997); U: uncertain; S: same star as SMC\_SC10 128768

Table 2  
FO/SO Double-Mode Cepheids in the SMC

Field	Star No.	RA(J2000)	DEC(J2000)	$P_{\text{SO}}$ [days]	$R_{21}^{\text{SO}}$	$\phi_{21}^{\text{SO}}$	$P_{\text{FO}}$ [days]	$R_{21}^{\text{FO}}$	$\phi_{21}^{\text{FO}}$	$P_{\text{SO}}/P_{\text{FO}}$	$I$ [mag]	$B - V$ [mag]	$V - I$ [mag]	Remarks
SMC_SC1	20157	0 <sup>h</sup> 36 <sup>m</sup> 51 <sup>s</sup> .24	-73°14'42".4	0.68762	0.130	5.375	0.85458	0.300	4.093	0.80463	16.950	0.332	0.529	M
SMC_SC2	14736	0 <sup>h</sup> 39 <sup>m</sup> 35 <sup>s</sup> .04	-73°13'00".6	0.54069	0.000	-	0.67043	0.239	4.005	0.80648	17.194	0.319	0.503	
SMC_SC2	19900	0 <sup>h</sup> 39 <sup>m</sup> 33 <sup>s</sup> .70	-73°01'27".0	0.54438	0.124	4.877	0.67490	0.256	3.948	0.80661	17.249	0.235	0.569	M
SMC_SC2	31653	0 <sup>h</sup> 40 <sup>m</sup> 34 <sup>s</sup> .96	-73°30'03".9	0.57816	0.000	-	0.71748	0.314	3.819	0.80582	17.298	0.376	0.534	
SMC_SC2	46920	0 <sup>h</sup> 40 <sup>m</sup> 27 <sup>s</sup> .29	-72°59'51".0	0.54367	0.161	5.585	0.67460	0.250	3.636	0.80591	17.442	0.407	0.595	
SMC_SC2	97203	0 <sup>h</sup> 42 <sup>m</sup> 13 <sup>s</sup> .29	-73°13'09".9	0.67717	0.121	4.190	0.84264	0.275	4.102	0.80363	17.233	0.422	0.641	M
SMC_SC3	20080	0 <sup>h</sup> 42 <sup>m</sup> 56 <sup>s</sup> .00	-73°18'25".1	0.56937	0.185	2.793	0.70585	0.283	3.948	0.80664	17.458	0.358	0.579	M
SMC_SC3	35943	0 <sup>h</sup> 43 <sup>m</sup> 08 <sup>s</sup> .17	-73°03'40".9	0.54626	0.257	4.475	0.67706	0.197	3.638	0.80681	17.595	0.420	0.590	M
SMC_SC3	115945	0 <sup>h</sup> 44 <sup>m</sup> 29 <sup>s</sup> .18	-73°33'42".8	0.63146	0.244	1.151	0.78528	0.276	3.878	0.80412	17.293	0.354	0.528	U
SMC_SC4	2356	0 <sup>h</sup> 46 <sup>m</sup> 03 <sup>s</sup> .39	-73°31'08".8	0.55699	0.399	3.116	0.69077	0.218	3.760	0.80633	17.295	0.367	0.508	
SMC_SC4	8429	0 <sup>h</sup> 45 <sup>m</sup> 49 <sup>s</sup> .47	-73°23'45".0	0.52784	0.000	-	0.65506	0.191	3.537	0.80579	17.276	0.316	0.518	
SMC_SC4	82181	0 <sup>h</sup> 46 <sup>m</sup> 46 <sup>s</sup> .74	-72°58'37".4	0.50404	0.129	4.993	0.62485	0.233	3.680	0.80666	17.423	0.386	0.521	
SMC_SC4	101292	0 <sup>h</sup> 47 <sup>m</sup> 20 <sup>s</sup> .96	-73°31'26".3	0.66873	0.174	5.128	0.83097	0.306	4.010	0.80476	17.045	0.387	0.554	M
SMC_SC4	106956	0 <sup>h</sup> 47 <sup>m</sup> 08 <sup>s</sup> .11	-73°23'54".8	0.59592	0.000	-	0.73921	0.324	3.989	0.80616	16.867	0.378	0.559	M
SMC_SC4	106992	0 <sup>h</sup> 47 <sup>m</sup> 37 <sup>s</sup> .88	-73°22'42".4	1.05622	0.140	5.233	1.31230	0.153	3.756	0.80486	16.639	0.544	0.724	
SMC_SC4	110510	0 <sup>h</sup> 47 <sup>m</sup> 15 <sup>s</sup> .10	-73°20'19".2	0.49322	0.000	-	0.61132	0.237	3.644	0.80681	17.568	0.486	0.574	U
SMC_SC4	131229	0 <sup>h</sup> 47 <sup>m</sup> 10 <sup>s</sup> .49	-72°58'44".0	0.80409	0.241	5.499	1.00283	0.185	4.164	0.80182	17.006	0.525	0.668	
SMC_SC4	150011	0 <sup>h</sup> 48 <sup>m</sup> 00 <sup>s</sup> .07	-73°31'50".5	0.49172	0.168	4.639	0.60983	0.281	3.602	0.80632	17.363	0.332	0.491	M
SMC_SC4	150103	0 <sup>h</sup> 47 <sup>m</sup> 58 <sup>s</sup> .87	-73°30'00".9	0.52885	0.000	-	0.65650	0.255	3.634	0.80556	17.539	0.335	0.574	
SMC_SC4	153342	0 <sup>h</sup> 48 <sup>m</sup> 10 <sup>s</sup> .79	-73°27'50".6	0.57542	0.232	3.596	0.71429	0.314	3.883	0.80558	17.355	0.452	0.645	
SMC_SC4	163672	0 <sup>h</sup> 48 <sup>m</sup> 32 <sup>s</sup> .10	-73°18'02".1	0.46360	0.000	-	0.57435	0.130	3.036	0.80717	17.705	0.432	0.625	U
SMC_SC4	171521	0 <sup>h</sup> 48 <sup>m</sup> 05 <sup>s</sup> .44	-73°09'54".5	0.54163	0.182	4.569	0.67212	0.266	3.619	0.80585	17.586	0.278	0.824	
SMC_SC4	182628	0 <sup>h</sup> 48 <sup>m</sup> 03 <sup>s</sup> .42	-73°00'06".8	0.77097	0.000	-	0.95956	0.245	4.023	0.80346	16.813	0.430	0.605	
SMC_SC4	186443	0 <sup>h</sup> 48 <sup>m</sup> 22 <sup>s</sup> .25	-72°55'10".3	0.62631	0.000	-	0.77443	0.232	3.253	0.80874	16.827	0.654	0.874	

Table 2

Continued

Field	Star No.	RA(J2000)	DEC(J2000)	$P_{\text{SO}}$ [days]	$R_{21}^{\text{SO}}$	$\phi_{21}^{\text{SO}}$	$P_{\text{FO}}$ [days]	$R_{21}^{\text{FO}}$	$\phi_{21}^{\text{FO}}$	$P_{\text{SO}}/P_{\text{FO}}$	$I$ [mag]	$B - V$ [mag]	$V - I$ [mag]	Remarks
SMC_SC5	16449	0 <sup>h</sup> 48 <sup>m</sup> 49 <sup>s</sup> .02	-73°19′45″.3	0.56769	0.154	5.339	0.70421	0.184	3.934	0.80614	17.307	0.396	0.584	
SMC_SC5	70168	0 <sup>h</sup> 48 <sup>m</sup> 59 <sup>s</sup> .17	-72°44′01″.2	0.53037	0.168	5.234	0.65810	0.236	3.636	0.80591	17.346	-	0.510	M
SMC_SC5	129596	0 <sup>h</sup> 49 <sup>m</sup> 27 <sup>s</sup> .36	-72°59′36″.6	0.60638	0.175	5.034	0.75250	0.267	3.837	0.80582	17.389	0.424	0.619	
SMC_SC5	170398	0 <sup>h</sup> 50 <sup>m</sup> 02 <sup>s</sup> .33	-73°23′09″.1	0.67750	0.127	4.252	0.84209	0.234	4.034	0.80455	16.817	0.448	0.579	
SMC_SC5	230217	0 <sup>h</sup> 50 <sup>m</sup> 43 <sup>s</sup> .97	-72°44′42″.4	0.89780	0.089	1.756	1.11558	0.215	4.027	0.80478	16.487	0.417	0.605	
SMC_SC5	235353	0 <sup>h</sup> 50 <sup>m</sup> 46 <sup>s</sup> .00	-72°40′58″.0	0.60191	0.122	4.920	0.74684	0.312	3.762	0.80594	17.061	0.329	0.497	
SMC_SC5	240099	0 <sup>h</sup> 51 <sup>m</sup> 21 <sup>s</sup> .55	-73°35′48″.6	0.51894	0.154	6.043	0.64238	0.250	3.421	0.80784	17.588	0.409	0.623	
SMC_SC5	266081	0 <sup>h</sup> 51 <sup>m</sup> 13 <sup>s</sup> .77	-73°14′03″.7	0.70446	0.000	-	0.87304	0.172	3.808	0.80690	16.986	0.511	0.651	
SMC_SC5	289174	0 <sup>h</sup> 50 <sup>m</sup> 55 <sup>s</sup> .83	-73°00′13″.5	0.58283	0.000	-	0.72293	0.178	4.176	0.80621	17.618	0.480	0.714	
SMC_SC5	294824	0 <sup>h</sup> 51 <sup>m</sup> 20 <sup>s</sup> .94	-72°58′04″.1	0.59290	0.117	4.132	0.73505	0.189	3.932	0.80661	17.124	0.410	0.610	
SMC_SC5	306011	0 <sup>h</sup> 51 <sup>m</sup> 00 <sup>s</sup> .90	-72°51′00″.9	0.66677	0.182	4.616	0.82864	0.282	4.116	0.80466	17.253	0.507	0.693	
SMC_SC5	306021	0 <sup>h</sup> 51 <sup>m</sup> 16 <sup>s</sup> .95	-72°50′41″.5	0.61124	0.000	-	0.75929	0.270	3.873	0.80502	17.086	0.386	0.577	
SMC_SC6	17580	0 <sup>h</sup> 52 <sup>m</sup> 10 <sup>s</sup> .34	-73°13′19″.8	0.61781	0.138	3.783	0.76693	0.243	3.791	0.80556	17.316	0.382	0.614	
SMC_SC6	129043	0 <sup>h</sup> 52 <sup>m</sup> 55 <sup>s</sup> .42	-72°59′18″.4	0.57559	0.174	2.933	0.71391	0.247	4.019	0.80625	17.297	0.381	0.521	M
SMC_SC6	158249	0 <sup>h</sup> 52 <sup>m</sup> 33 <sup>s</sup> .94	-72°42′59″.5	0.58160	0.191	5.903	0.72200	0.271	4.036	0.80554	17.322	0.412	0.564	
SMC_SC6	180332	0 <sup>h</sup> 53 <sup>m</sup> 08 <sup>s</sup> .57	-73°20′48″.6	0.49649	0.271	4.936	0.61415	0.208	3.003	0.80842	17.455	0.386	0.582	
SMC_SC6	190505	0 <sup>h</sup> 53 <sup>m</sup> 44 <sup>s</sup> .61	-73°12′53″.6	0.58669	0.278	4.001	0.72834	0.207	3.877	0.80552	17.417	0.397	0.643	M
SMC_SC6	195011	0 <sup>h</sup> 53 <sup>m</sup> 39 <sup>s</sup> .36	-73°09′20″.8	0.57939	0.235	3.695	0.71930	0.264	3.904	0.80549	17.219	0.353	0.506	
SMC_SC6	246813	0 <sup>h</sup> 53 <sup>m</sup> 22 <sup>s</sup> .73	-72°35′21″.3	0.59226	0.186	5.867	0.73479	0.198	3.997	0.80603	17.150	0.145	0.699	
SMC_SC6	251147	0 <sup>h</sup> 53 <sup>m</sup> 15 <sup>s</sup> .96	-72°31′31″.9	0.58204	0.000	-	0.72241	0.283	3.973	0.80569	17.235	0.316	0.581	
SMC_SC6	277080	0 <sup>h</sup> 54 <sup>m</sup> 04 <sup>s</sup> .94	-73°05′51″.1	0.87847	0.146	4.739	1.09587	0.199	4.110	0.80162	16.610	0.363	0.627	
SMC_SC6	291809	0 <sup>h</sup> 54 <sup>m</sup> 08 <sup>s</sup> .59	-72°56′33″.8	0.50853	0.244	4.268	0.63070	0.225	3.621	0.80629	17.362	0.326	0.547	
SMC_SC7	4204	0 <sup>h</sup> 54 <sup>m</sup> 49 <sup>s</sup> .93	-73°15′00″.6	0.59049	0.151	6.019	0.73323	0.230	3.871	0.80533	17.182	0.479	0.525	
SMC_SC7	8786	0 <sup>h</sup> 55 <sup>m</sup> 03 <sup>s</sup> .01	-73°13′59″.0	0.66904	0.195	3.887	0.83081	0.218	4.031	0.80529	17.136	0.341	0.562	

Table 2

Concluded

Field	Star No.	RA(J2000)	DEC(J2000)	$P_{\text{SO}}$ [days]	$R_{21}^{\text{SO}}$	$\phi_{21}^{\text{SO}}$	$P_{\text{FO}}$ [days]	$R_{21}^{\text{FO}}$	$\phi_{21}^{\text{FO}}$	$P_{\text{SO}}/P_{\text{FO}}$	$I$ [mag]	$B - V$ [mag]	$V - I$ [mag]	Remarks
SMC_SC7	42358	0 <sup>h</sup> 54 <sup>m</sup> 59 <sup>s</sup> .19	-72°47'15''.2	0.68167	0.348	4.576	0.84817	0.281	3.938	0.80370	17.169	0.450	0.598	
SMC_SC7	100561	0 <sup>h</sup> 55 <sup>m</sup> 36 <sup>s</sup> .76	-73°00'33''.8	0.68260	0.234	5.493	0.84935	0.265	4.054	0.80367	16.897	0.454	0.620	
SMC_SC7	133650	0 <sup>h</sup> 55 <sup>m</sup> 54 <sup>s</sup> .58	-72°32'30''.7	0.62520	0.000	-	0.77637	0.287	3.881	0.80529	17.291	0.386	0.600	
SMC_SC7	137641	0 <sup>h</sup> 55 <sup>m</sup> 50 <sup>s</sup> .22	-72°31'18''.7	0.52324	0.161	4.203	0.64867	0.300	3.731	0.80664	17.228	0.391	0.484	
SMC_SC8	30693	0 <sup>h</sup> 57 <sup>m</sup> 57 <sup>s</sup> .62	-72°38'08''.3	0.57695	0.000	-	0.71541	0.246	3.699	0.80646	17.490	0.531	0.634	M
SMC_SC8	52895	0 <sup>h</sup> 57 <sup>m</sup> 47 <sup>s</sup> .19	-72°18'03''.5	0.68079	0.210	0.065	0.84470	0.214	3.376	0.80595	16.792	0.375	0.579	
SMC_SC8	62881	0 <sup>h</sup> 58 <sup>m</sup> 49 <sup>s</sup> .63	-73°00'52''.3	0.66639	0.126	4.419	0.82868	0.251	4.045	0.80416	17.286	0.477	0.604	
SMC_SC8	66186	0 <sup>h</sup> 58 <sup>m</sup> 21 <sup>s</sup> .52	-72°58'50''.5	0.64056	0.000	-	0.79688	0.299	3.952	0.80383	17.230	0.360	0.585	U
SMC_SC8	94606	0 <sup>h</sup> 58 <sup>m</sup> 50 <sup>s</sup> .10	-72°31'41''.3	0.71048	0.126	4.934	0.88413	0.283	4.040	0.80359	17.321	0.456	0.705	
SMC_SC8	113418	0 <sup>h</sup> 58 <sup>m</sup> 59 <sup>s</sup> .34	-73°05'00''.3	0.45432	0.000	-	0.56318	0.262	3.511	0.80670	17.694	0.331	0.524	
SMC_SC8	122864	0 <sup>h</sup> 59 <sup>m</sup> 11 <sup>s</sup> .91	-72°55'18''.3	0.56490	0.165	4.601	0.70033	0.215	3.670	0.80662	17.337	0.490	0.559	M
SMC_SC8	139476	0 <sup>h</sup> 59 <sup>m</sup> 13 <sup>s</sup> .40	-72°38'49''.4	0.70065	0.000	-	0.87091	0.268	3.918	0.80450	16.834	0.280	0.567	
SMC_SC8	186707	0 <sup>h</sup> 59 <sup>m</sup> 58 <sup>s</sup> .15	-72°42'14''.7	0.56577	0.120	4.302	0.70203	0.295	3.710	0.80591	17.507	0.386	0.658	
SMC_SC9	21140	1 <sup>h</sup> 00 <sup>m</sup> 59 <sup>s</sup> .27	-72°37'18''.6	0.50594	0.000	-	0.62729	0.245	3.791	0.80655	17.548	0.352	0.509	
SMC_SC9	47742	1 <sup>h</sup> 00 <sup>m</sup> 50 <sup>s</sup> .53	-72°04'43''.1	0.46623	0.000	-	0.57668	0.278	3.557	0.80847	17.463	-	0.542	
SMC_SC9	99881	1 <sup>h</sup> 02 <sup>m</sup> 19 <sup>s</sup> .78	-72°51'49''.9	0.49307	0.189	3.742	0.61126	0.261	3.776	0.80665	17.508	0.391	0.483	M
SMC_SC9	108504	1 <sup>h</sup> 02 <sup>m</sup> 07 <sup>s</sup> .98	-72°39'49''.0	0.49770	0.000	-	0.61713	0.258	3.604	0.80648	17.413	0.357	0.538	
SMC_SC10	85943	1 <sup>h</sup> 05 <sup>m</sup> 08 <sup>s</sup> .51	-72°40'04''.3	0.54366	0.000	-	0.67485	0.253	3.747	0.80560	17.253	0.303	0.543	U
SMC_SC10	124862	1 <sup>h</sup> 05 <sup>m</sup> 50 <sup>s</sup> .28	-72°29'34''.9	0.58766	0.000	-	0.72949	0.264	4.004	0.80558	17.136	0.366	0.569	
SMC_SC10	128831	1 <sup>h</sup> 06 <sup>m</sup> 17 <sup>s</sup> .31	-72°22'01''.6	0.59299	0.184	4.832	0.73599	0.252	3.896	0.80570	17.271	0.434	0.614	
SMC_SC11	13365	1 <sup>h</sup> 06 <sup>m</sup> 34 <sup>s</sup> .76	-72°41'04''.4	0.51491	0.277	4.191	0.63875	0.169	3.750	0.80612	17.236	0.358	0.493	
SMC_SC11	24118	1 <sup>h</sup> 06 <sup>m</sup> 17 <sup>s</sup> .30	-72°22'01''.7	0.59286	0.274	4.679	0.73597	0.234	3.919	0.80555	17.286	0.438	0.597	S
SMC_SC11	42383	1 <sup>h</sup> 07 <sup>m</sup> 37 <sup>s</sup> .33	-72°45'50''.6	0.64988	0.117	3.905	0.80714	0.270	3.700	0.80516	17.128	0.353	0.575	

Remarks: M: Double-mode Cepheid reported by MACHO (Alcock *et al.* 1997); U: uncertain; S: same star as SMC\_SC10 128831

sators, respectively. The first and second columns in each Appendix contain original photometric data folded with the shorter and longer periods while the remaining columns show variability attributed to each mode after subtraction of the other period variability approximated by Fourier series of fifth order. For objects revealing also periodicity equal to the sum and/or difference of both mode frequencies and having an amplitude larger than twice the formal error – such terms were also subtracted from the original data. *BVI* photometry of all objects will be available from the OGLE Internet archive when the catalog of Cepheids in the SMC is released.

Completeness of the sample is determined by completeness of the variable star search in the OGLE databases and efficiency of double-mode Cepheid detection algorithm. Completeness of the OGLE variable stars catalog was already estimated for eclipsing stars which are much more difficult to detect. For objects brighter than  $I = 17$  it is likely to be higher than 90% (Udalski *et al.* 1998b). For stars as bright and easy to detect as Cepheids it should be similar or even higher. Completeness of the detection algorithm can be assessed by comparison of results obtained in the preliminary and final (CLEAN) searches. More than 90% objects in both lists are common suggesting good completeness of the search.

As a test of completeness we cross-identified double mode Cepheids reported by MACHO (Alcock *et al.* 1997). 19 out of 20 objects which are located in the OGLE fields were detected during our search. They are marked by letter 'M' in the last column of Tables 1 and 2. The remaining object, MACHO\*00:57:27.0-73:04:39, was also analyzed but it seems to be a single period Cepheid.

## 5 Discussion

93 double-mode Cepheids were identified during the presented search in the 2.4 square degree area of the central bar of the SMC. 23 objects pulsate simultaneously in the fundamental mode and first overtone while 70 objects in the first and second overtones. The sample constitutes the most numerous sample of double-mode Cepheids located in one environment. Completeness of the sample is high, likely larger than 90%.

### 5.1 Period Ratio in Double-Mode Cepheids

Fig. 1 presents the ratio of periods of the FU/FO and FO/SO pulsators plotted as a function of the lower mode period. In both cases a clear dependence

on the period is seen, similarly to the Galactic and LMC Cepheids (Alcock *et al.* 1995). More numerous sample allows for more precise approximation of that dependence. The best linear fits are as follows:

FU/FO:

$$\frac{P_{\text{FO}}}{P_{\text{FU}}} = \frac{0.741}{0.001} - \frac{0.032}{0.005} \times \log P_{\text{FU}}, \quad (1)$$

FO/SO:

$$\frac{P_{\text{SO}}}{P_{\text{FO}}} = \frac{0.804}{0.001} - \frac{0.014}{0.002} \times \log P_{\text{FO}}. \quad (2)$$

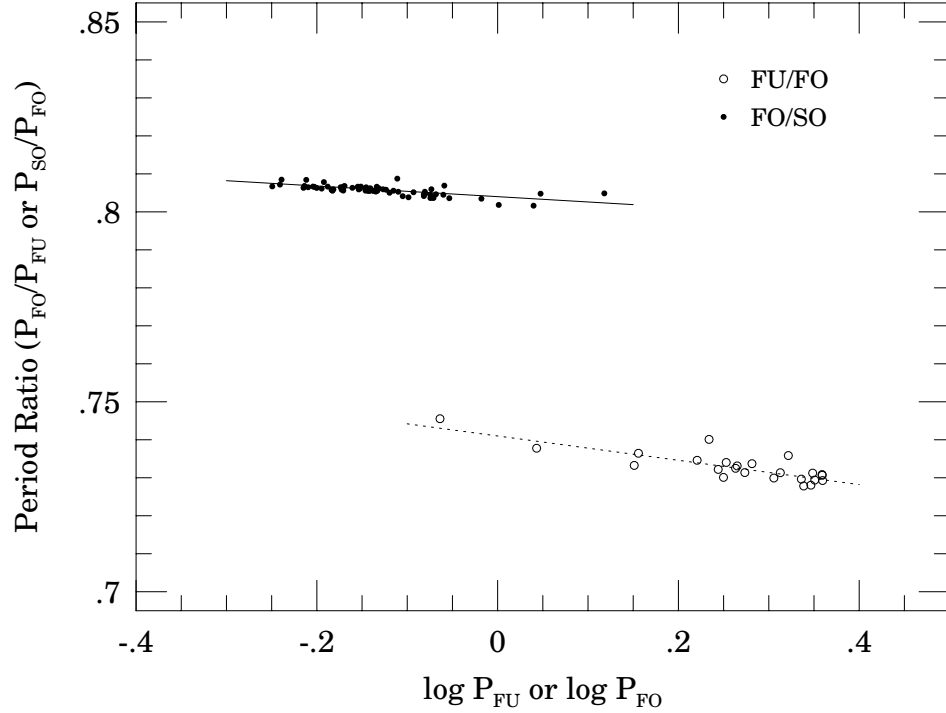


Fig. 1. Ratio of periods in double-mode Cepheids plotted as a function of the longer period. Dotted and solid lines mark the best linear fits given by Eqs. 1 and 2, respectively.

Comparison of coefficients in Eqs. (1) and (2) with similar ones for the Galactic and LMC double-mode Cepheids indicates that the ratio of periods for FU/FO pulsators is slightly larger for the SMC Cepheids than for the LMC and Galactic objects which are more metal rich. On the other hand the ratio for FO/SO objects is almost identical with the ratio of the LMC objects but the slope of the relation is flatter.

## 5.2 Fourier Decomposition of Light Curves of Double-Mode Cepheids

Fourier decomposition of light curves of pulsating stars has been widely used for analyzing their properties (Simon and Lee 1981). In the case of Cepheids the ratio of amplitudes of the first harmonic and the fundamental period,  $R_{21} = A_2/A_1$ , and phase difference,  $\phi_{21} = \phi_2 - 2\phi_1$  are particularly useful. Both allow to distinguish between the fundamental mode and first overtone pulsators. The  $R_{21}$  vs.  $\log P$  diagram constructed for about 1400 Cepheids from the LMC (Alcock *et al.* 1999) shows two distinct and well separated "V-shape" sequences for Cepheids pulsating in the fundamental mode and the first overtone. In the similar diagram  $\phi_{21}$  vs.  $\log P$  the sequences for both modes of pulsation are also well defined but the separation is smaller and in some ranges of periods they overlap.

Fig. 2 presents the  $R_{21}$  vs.  $\log P$  and  $\phi_{21}$  vs.  $\log P$  diagrams constructed for about 2300 single-mode Cepheids (small dots) from the SMC. The Cepheids come from the preliminary catalog of Cepheids in the SMC, and therefore some very tiny contamination by non-Cepheid variable stars is still possible in these diagrams. Nevertheless both diagrams look basically the same as for the LMC Cepheids with well-separated "V-shape" sequences in the  $R_{21}$  vs.  $\log P$  diagram and two characteristic sequences in the  $\phi_{21}$  vs.  $\log P$  diagram.

To check behavior of double-mode Cepheids we decomposed their light curves to the sum of two Fourier series of fifth order corresponding to both periodicities including the terms of sum and difference of mode frequencies when their amplitudes were larger than twice the formal errors. Then we calculated  $R_{21}$  and  $\phi_{21}$  for both pulsating modes. They are listed in Tables 1 and 2.

Results for the FU/FO Cepheids are shown in Fig. 2: the values for the fundamental mode pulsation are plotted with large filled dots while for the first overtone mode mode with open circles. Objects with non-significant first harmonic amplitude,  $A_2$ , (*i.e.*, with almost sinusoidal light curve) have  $R_{21} = 0$  and their  $\phi_{21}$  is not defined.

The main conclusion which can be drawn from Fig. 2 is that while the first overtone pulsations usually dominate in this class of double-mode Cepheids and their  $R_{21}$  and  $\phi_{21}$  fall in the sequences of the single-mode first overtone pulsators, the fundamental mode pulsations have  $R_{21}$  values much smaller than corresponding single-mode fundamental mode Cepheids. This means that the fundamental mode pulsations in double-mode Cepheids are

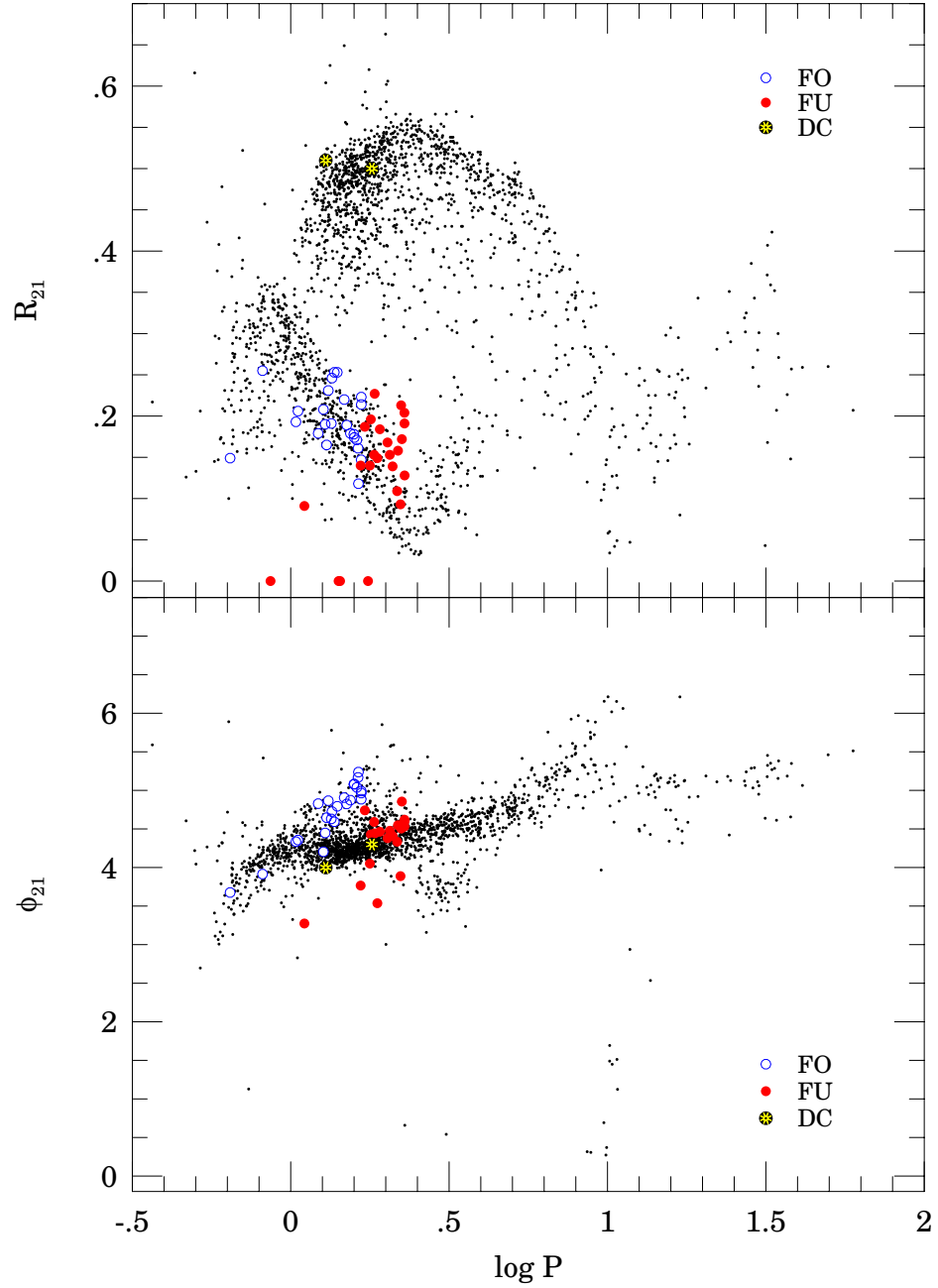


Fig. 2.  $R_{21}$  and  $\phi_{21}$  vs.  $\log P$  diagrams for single-mode Cepheids from the SMC (small dots). Large open and filled circles mark values of the first overtone and fundamental mode pulsations in the FU/FO double-mode Cepheids, respectively. Star symbols denote values of  $R_{21}$  and  $\phi_{21}$  for "double Cepheid", SMC\_SC5 208044.

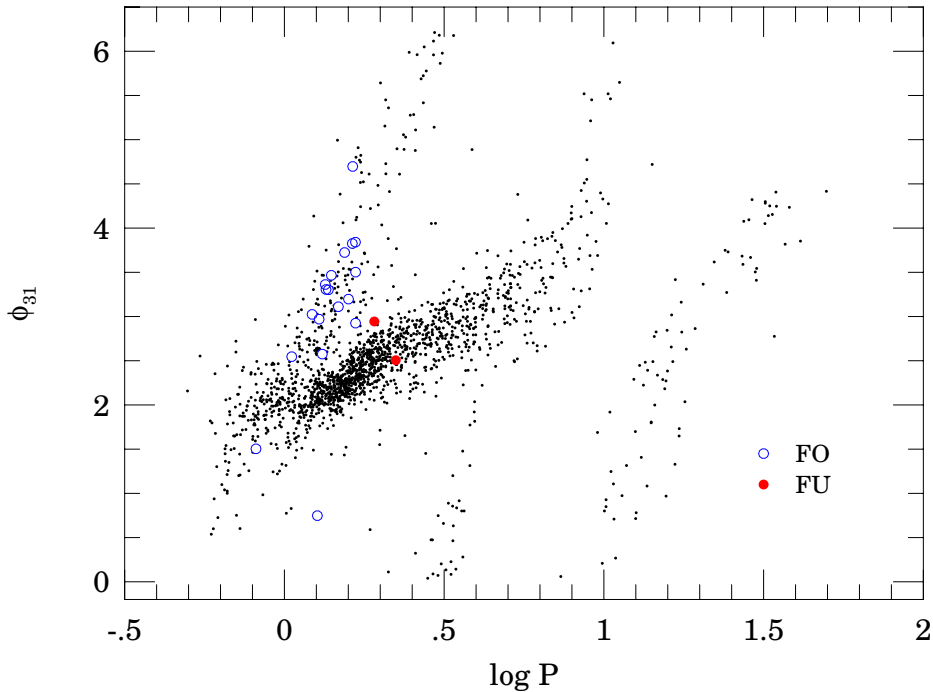


Fig. 3.  $\phi_{31}$  vs.  $\log P$  diagram for single-mode Cepheids from the SMC (small dots). Large open and filled circles mark values of the first overtone and fundamental mode pulsations in the FU/FO double-mode Cepheids, respectively.

suppressed making the light curve not that sharp and more sinusoidal than for single-mode Cepheids of that type. In the most extreme cases the fundamental mode pulsations are low amplitude almost sinusoidal variations (see Appendix B).

$\phi_{21}$  values of the fundamental mode pulsations in double-mode Cepheids seem to fall largely in the fundamental mode Cepheid sequence. Unfortunately, in this part of the  $\phi_{21}$  vs.  $\log P$  diagram the sequences of fundamental mode and first overtone Cepheids overlap. Therefore the diagram is not fully conclusive.

Mantegazza and Poretti (1992) suggested that the phase difference of the second harmonic and fundamental period,  $\phi_{31} = \phi_3 - 3\phi_1$  might be better for discrimination between the first overtone and fundamental mode pulsating objects. The sequences for the first overtone and fundamental mode Cepheids are better separated in the  $\phi_{31}$  vs.  $\log P$  than in the  $\phi_{21}$  vs.  $\log P$  diagram. Therefore we constructed the  $\phi_{31}$  vs.  $\log P$  diagram for all single-mode Cepheids with statistically significant second harmonic ampli-

tude. The diagram is plotted in Fig. 3. Small dots represent single-mode Cepheids.

Indeed, two well separated sequences starting from approximately ( $\log P = 0, \phi_{31} = 2$ ) are clearly seen. The steeper one is populated by stars pulsating in the first overtone while the second one, more horizontal but rising rapidly at ( $\log P = 0.9, \phi_{31} = 4$ ) and better populated, by fundamental mode pulsators. The  $\phi_{31}$  values are periodic with the period equal to  $2\pi$  and they are shown in Fig. 3 in the range  $0 - 2\pi$ . Therefore two additional sequences starting at ( $\log P = 0.5, \phi_{31} = 0$ ) and ( $\log P = 1.0, \phi_{31} = 0$ ) are simply continuation of the first overtone and fundamental mode Cepheid sequences, respectively.

We calculated the  $\phi_{31}$  values for all double-mode Cepheids of FU/FO type with statistically significant second harmonic amplitude. The values are listed in Table 1. Open circles in Fig. 3 mark positions of the first overtone pulsation values. As can be seen they fall well in the single-mode first overtone Cepheids sequence similar to the previous diagrams. Unfortunately, for the fundamental mode pulsations the  $\phi_{31}$  values could only be derived for two objects from the sample, SMC\_SC5 219993 and SMC\_SC7 57228 because the second harmonic amplitude is non-significant for the remaining Cepheids.  $\phi_{31}$  of these stars are plotted with filled dots in Fig. 3. Both values are located in the sequence of single-mode Cepheids pulsating in the fundamental mode. We may, thus, conclude that the longer period pulsations in the FU/FO double-mode Cepheids are indeed of the fundamental mode type in spite of the fact that their  $R_{21}$  is smaller as compared with values of single-mode objects in the  $R_{21}$  vs.  $\log P$  diagram.

Fig. 4 presents  $R_{21}$  vs.  $\log P$  and  $\phi_{21}$  vs.  $\log P$  diagrams for FO/SO double-mode Cepheids from the SMC. The first overtone pulsation values of  $R_{21}$  and  $\phi_{21}$  are plotted with large filled dots while those calculated for the second overtone pulsations with open circles.

The first overtone pulsations also dominate in this group of objects. Their  $R_{21}$  and  $\phi_{21}$  values are located exactly in the corresponding sequences of the single-mode first overtone Cepheids. The second overtone pulsations are typically low amplitude quasi sinusoidal light variations (see Appendix C). For many objects the first harmonic amplitude,  $A_2$ , of the second overtone period is not statistically significant (*i.e.*,  $R_{21} = 0$ ), while for the remaining ones it is usually very small, making  $R_{21}$  small, typically below 0.2. The  $\phi_{21}$  values for the second overtone pulsations are usually larger than those corresponding to the first overtone sequence providing a way to distinguish between those two modes of pulsations.

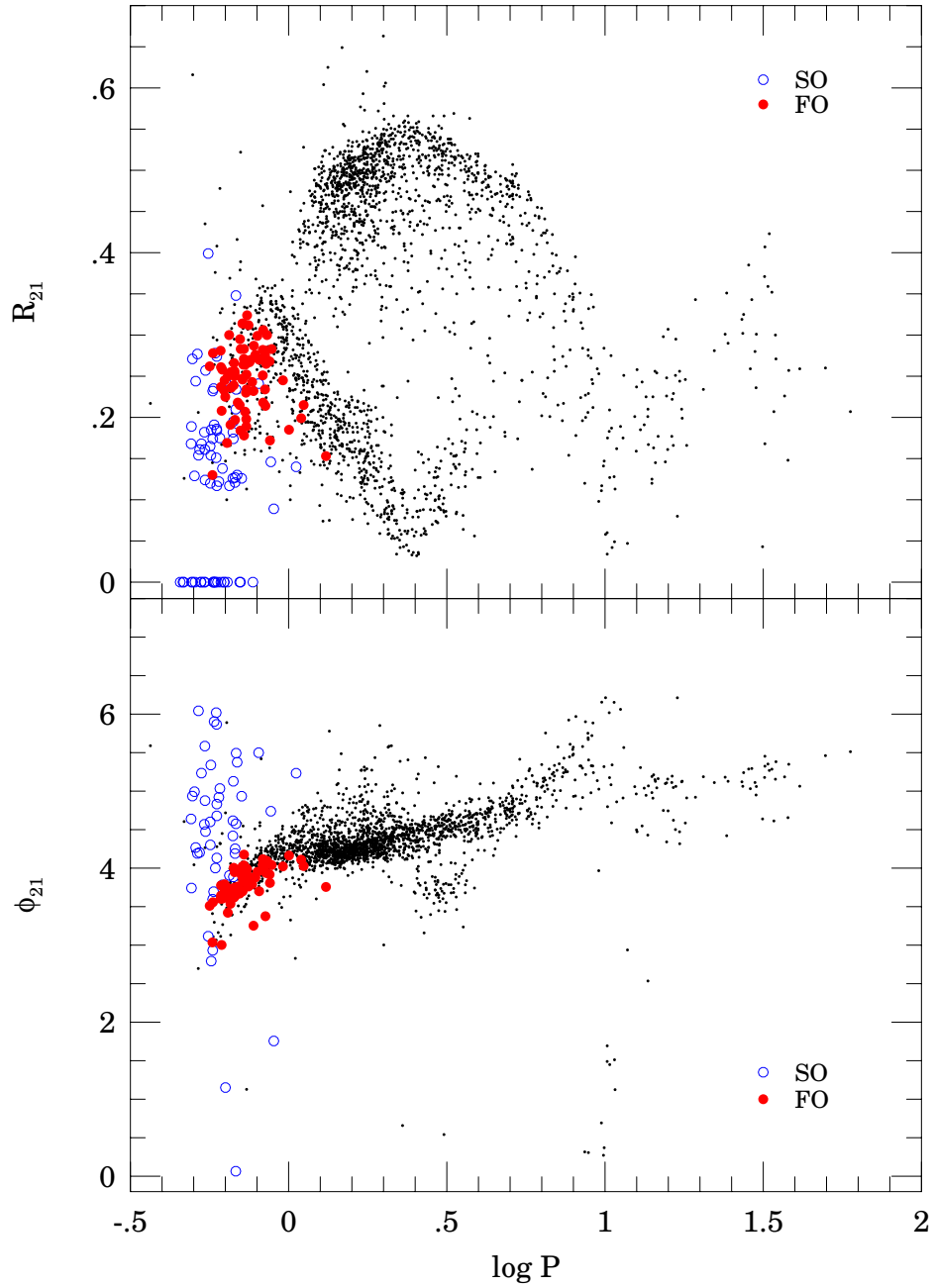


Fig. 4.  $R_{21}$  and  $\phi_{21}$  vs.  $\log P$  diagrams for single-mode Cepheids from the SMC (small dots). Large open and filled circles mark values of the second and first overtone pulsations in the FO/SO double-mode Cepheids, respectively.

### 5.3 Colors of Double-Mode Cepheids

Huge and homogeneous sample of Cepheids in the observed region of the SMC and relatively small extinction toward the SMC makes it possible to analyze distribution of color indices of different types of Cepheids in the SMC, that is the temperature distribution of different mode pulsators.

We selected four classes of Cepheids: single-mode fundamental and first overtone pulsators and double-mode FU/FO and FO/SO objects. The single-mode stars were divided into the first overtone and fundamental mode groups based on location in the  $R_{21}$  vs.  $\log P$  and period-luminosity ( $\langle I \rangle$  vs.  $\log P$ ) diagrams. These samples included 705 and 1148 objects, respectively.

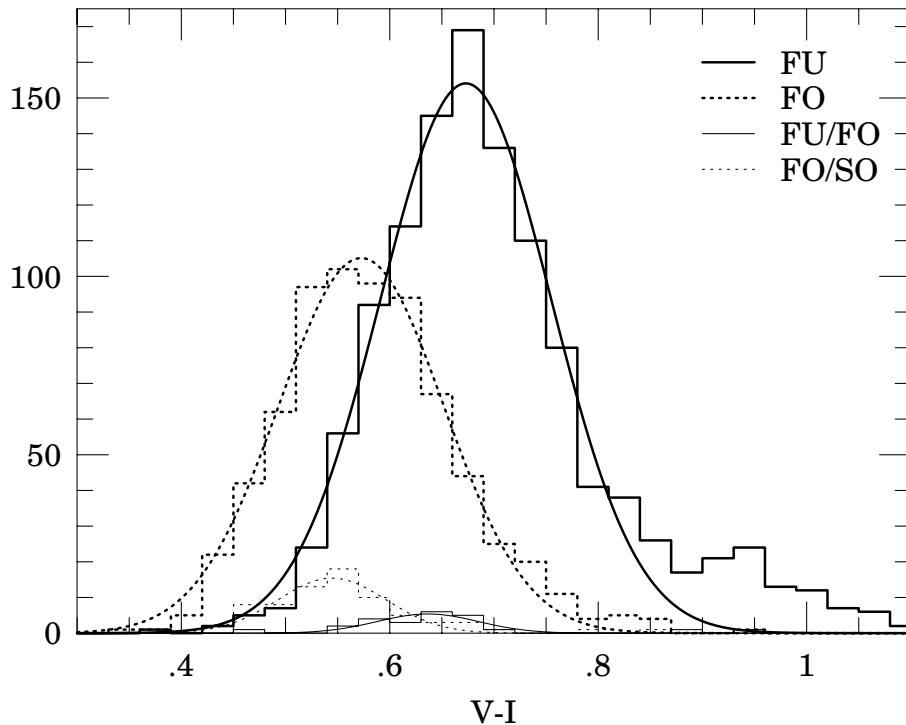


Fig. 5. Histograms of  $V - I$  color distribution of single-mode and double-mode Cepheids in the SMC. Thick lines represent distribution of single-mode Cepheids: solid line – fundamental mode pulsators, dotted line – first overtone objects. Distribution of double-mode Cepheids is marked by thin line: solid line – FU/FO stars, dotted line – FO/SO Cepheids. The bins are 0.03 mag wide.

For all objects the mean, intensity weighted magnitudes in the  $V$  and  $I$ -bands were calculated. Then the magnitudes of objects from fields SMC\_SC2–

SMC\_SC11 were corrected for difference of the mean reddening between the field in which a given object is located and the mean reddening in the SMC\_SC1 field. The mean difference of reddening between SMC\_SC1 and the remaining fields was derived based on the mean difference of the  $I$ -band magnitudes of the red clump stars in corresponding fields. The mean  $I$ -band magnitude of the red clump stars is a good reference of brightness, particularly in homogeneous environment like central parts of the SMC (Udalski 1998a,b). Thus magnitudes of all Cepheids were tied to the reference field SMC\_SC1. The mean extinction of the latter field is  $A_I = 0.11$  mag, corresponding to  $E(B - V) = 0.06$  and  $E(V - I) = 0.08$ , based on the mean  $I$ -band magnitude of the red clump stars,  $I = 18.457$ , and the mean extinction free magnitude of the red clump stars in the SMC (Udalski 1998a,b).

Fig. 5 shows histograms of  $(V - I)$  color index of all four groups of Cepheids. The width of the bin is 0.03 mag. Thick solid and dotted lines correspond to the single-mode fundamental and first overtone Cepheids while thin solid and dotted lines to the FU/FO and FO/SO double-mode Cepheids. All histograms were fitted with a Gaussian which fits well observed color distributions. In the case of single-mode fundamental mode Cepheids there is a small excess of red objects caused by the redward bending of the instability strip for the brightest stars. This effect is only important for single-mode fundamental type Cepheids with long periods.

The mean  $V - I$  color and the standard deviation of its distribution are 0.673, 0.08 and 0.573, 0.08 for single-mode fundamental and first overtone Cepheids, respectively. For FU/FO and FO/SO double-mode Cepheids the corresponding values are: 0.634, 0.05 and 0.545, 0.05, respectively. The single-mode first overtone Cepheids are on average by about 0.1 mag bluer than fundamental mode pulsators. As one could expect the FU/FO double-mode Cepheids have  $V - I$  color distribution in between the first and fundamental mode distribution of single-mode stars. The color distribution of FO/SO double-mode Cepheids resembles that of the single-mode first overtone stars but it is shifted bluewards.

#### 5.4 "Double Cepheid" in the SMC

The final search with the CLEAN algorithm was aimed at detection of double-mode Cepheids by constraining the searched periods to the range around the double-mode Cepheids period ratio. This approach omits, however, potential objects which are a Cepheid blended with another periodic object. For instance, three such cases of "double Cepheids" in the LMC were

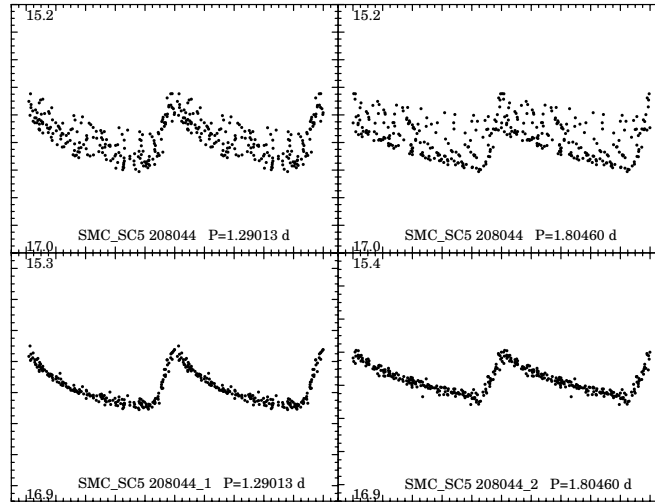


Fig. 6. Light curve of "double Cepheid", SMC\_SC5 208044. The upper panels show the original data folded with two detected periods while the lower panels the light curve of each component after subtraction of variability of the second star approximated by Fourier series of fifth order.

reported by Alcock *et al.* (1995). To look for similar objects in the SMC we reran our searching procedure with another constraint, namely only stars with the second peak in the power spectrum (third if the second peak was the harmonic of the most prominent one, etc), with frequency outside the double-mode Cepheid range and higher than one fourth of the first peak power were selected.

One object from this sample, SMC\_SC5 208044 (RA(J2000) =  $0^{\text{h}}50^{\text{m}}38^{\text{s}}78$ , DEC(J2000) =  $-72^{\circ}59'02''.1$ ), seems to consist of two blended Cepheids. Fig. 6 shows the light curves of both components of the blend. The finding chart is shown in Fig. 7.

Both components seem to be fundamental mode pulsators and although their period ratio is close to the double-mode Cepheid range, the shape of the light curves of both components and Fourier parameters marked in Fig. 2 by star symbols leave little doubts that they are two distinct, blended objects. Such an interpretation is also supported by larger brightness of the star than other objects of similar period and also lack of periodicity corresponding to the sum and difference of two detected frequencies which in a double-mode Cepheid of such a large amplitude should be easily detectable.

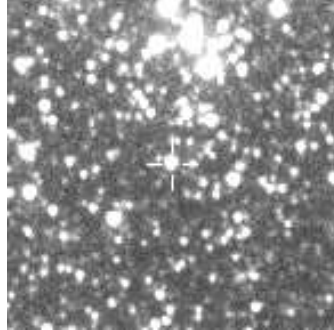


Fig. 7. Finding chart of the "double Cepheid", SMC\_SC5 208044. Size of the *I*-band subframe is  $60 \times 60$  arcsec. North is up and East to the left.

It is impossible to conclude whether the system is only an optical blend or components are physically bounded. Spectroscopic observations could provide additional information to clear this problem.

**Acknowledgements.** The paper was partly supported by the Polish KBN grant 2P03D00814 to A. Udalski. Partial support for the OGLE project was provided with the NSF grant AST-9530478 to B. Paczyński.

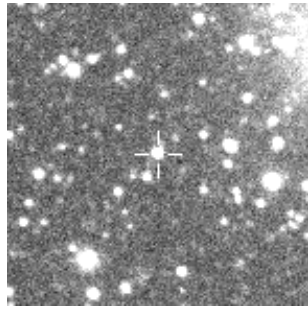
## REFERENCES

- Alcock, C. *et al.* 1995, *Astron. J.*, **109**, 1652.  
 Alcock, C. *et al.* 1997, astro-ph/9709025.  
 Alcock, C. *et al.* 1999, *Astrophys. J.*, **511**, 185.  
 Beaulieu, J.P. *et al.* 1997, *Astron. Astrophys.*, **321**, L5.  
 Mantegazza, L., and Poretti, E. 1992, *Astron. Astrophys.*, **261**, 137.  
 Pardo, I., and Poretti, E. 1997, *Astron. Astrophys.*, **324**, 121.  
 Roberts, D.H., Lehár, J., and Dreher, J.W. 1987, *Astron. J.*, **93**, 968.  
 Schwarzenberg-Czerny, A. 1989, *MNRAS*, **241**, 153.  
 Simon, N.R., and Lee, A.S. 1981, *Astrophys. J.*, **248**, 291.  
 Udalski, A., Kubiak, M., and Szymański, M. 1997, *Acta Astron.*, **47**, 319.  
 Udalski, A. 1998a, *Acta Astron.*, **48**, 113.  
 Udalski, A. 1998b, *Acta Astron.*, **48**, 383.  
 Udalski, A., Szymański, M., Kubiak, M., Pietrzyński, G., Woźniak, P., and Żebruń, K. 1998a, *Acta Astron.*, **48**, 147.  
 Udalski, A., Soszyński, I., Szymański, M., Kubiak, M., Pietrzyński, G., Woźniak, P., and Żebruń, K. 1998b, *Acta Astron.*, **48**, 563.

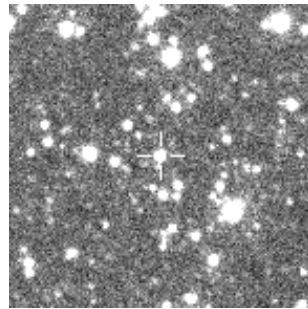
## Appendix A

### FU/FO Double-Mode Cepheids

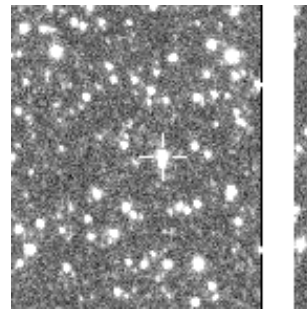
SMC\_SC1 35550



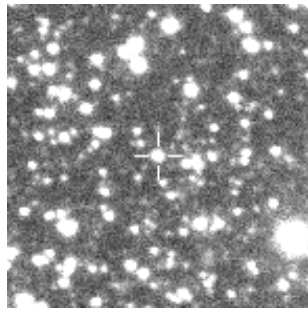
SMC\_SC1 60587



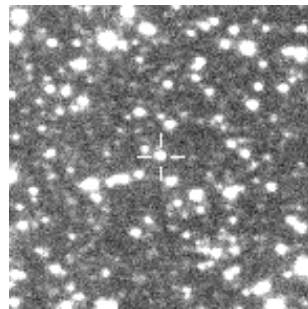
SMC\_SC2 61720



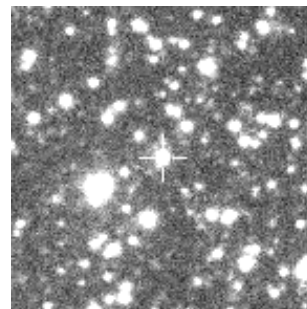
SMC\_SC4 56827



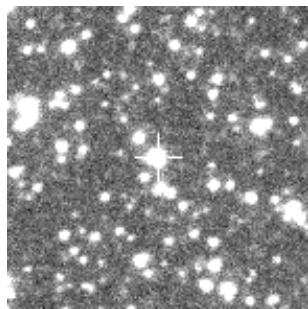
SMC\_SC4 75443



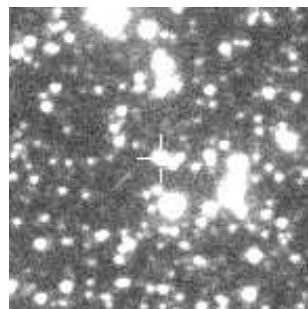
SMC\_SC4 91592



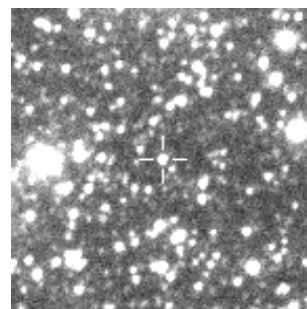
SMC\_SC4 145181



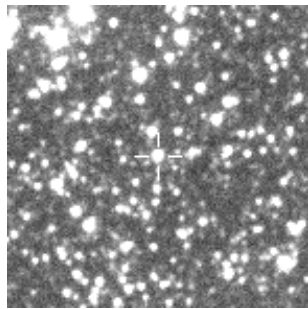
SMC\_SC4 175210



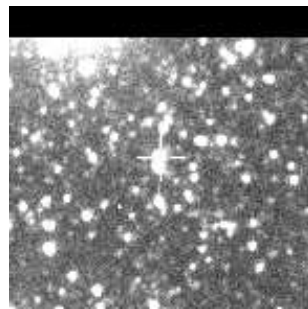
SMC\_SC5 38289



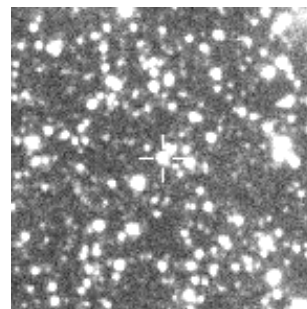
SMC\_SC5 117506



SMC\_SC5 155033



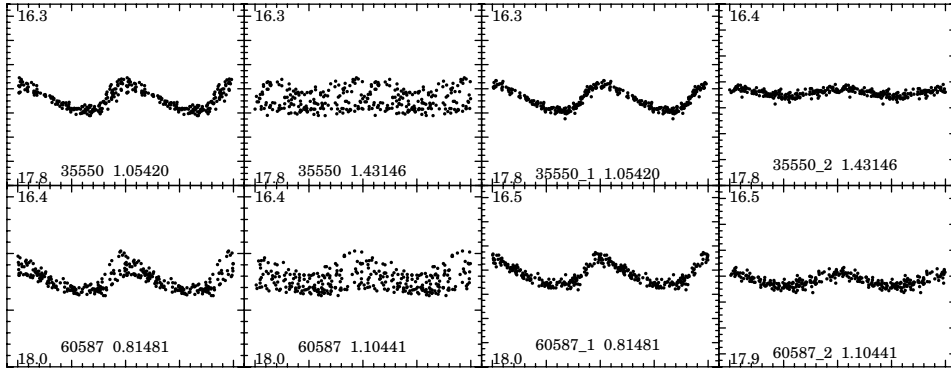
SMC\_SC5 219993



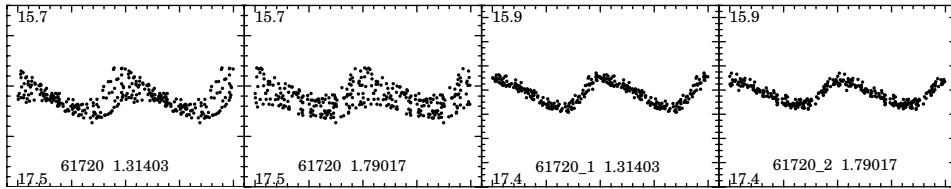
## Appendix B

### FU/FO Double-Mode Cepheids

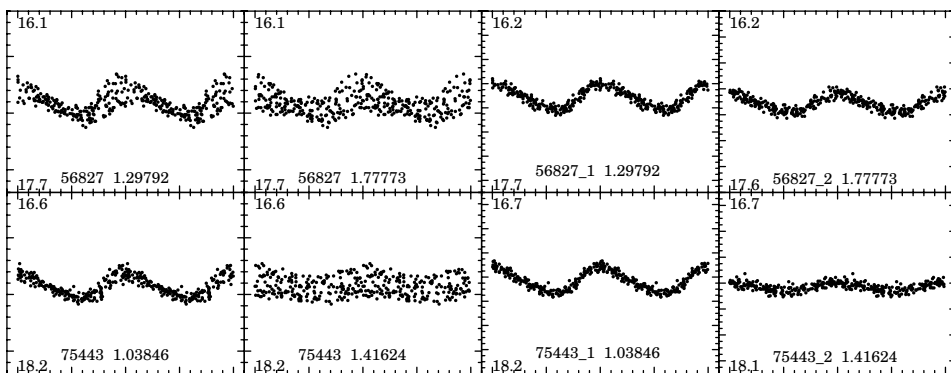
#### SMC\_SC1



#### SMC\_SC2



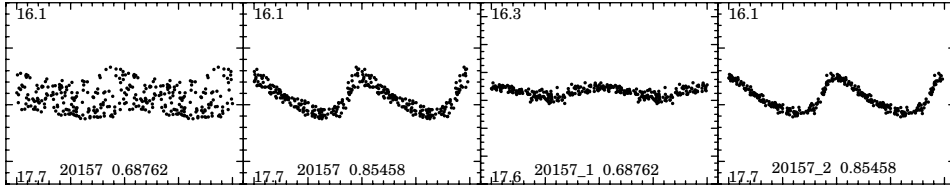
#### SMC\_SC4



# Appendix C

## FO/SO Double-Mode Cepheids

### SMC\_SC1



### SMC\_SC2

